

1

**A STUDY TO ASSESS THE EFFICACY OF
MAGNETIZATION TRANSFER RATIO IN DIFFERENTIATING
TUBERCULOMA FROM NEUROCYSTICERCOSIS**

**DISSERTATION SUBMITTED FOR
M.D. DEGREE EXAMINATION IN RADIO – DIAGNOSIS
BRANCH – VIII
MADRAS MEDICAL COLLEGE**



**THE TAMILNADU DR. M.G.R. MEDICAL UNIVERSITY
CHENNAI – TAMILNADU
INDIA
MARCH 2010**

CERTIFICATE

This is to certify that Dr. R. Ganga Devi has been a post graduate student during the period April 2008 to March 2010, in the Department of Radio diagnosis, Madras Medical College, Government General Hospital, Chennai.

This Dissertation titled, “A Study to Assess the Efficacy of Magnetization Transfer Ratio in differentiating Tuberculoma from Neurocysticercosis” is a bonafide work done by her during the study period and is being submitted to The Tamil nadu DR.M.G.R. Medical University, in partial fulfillment of the M.D. Branch VIII Radio diagnosis Examination.

DEAN

Madras Medical College,
Government General Hospital,
Chennai.

CERTIFICATE

This is to certify that Dr R Ganga Devi has been a post graduate student during the period April 2008 to March 2010, in the Department of Radio diagnosis, Madras Medical College, Government General Hospital, Chennai.

This Dissertation titled, “A Study to Assess the Efficacy of Magnetization Transfer Ratio in differentiating Tuberculoma from Neurocysticercosis” is a bonafide work done by her during the study period and is being submitted to The Tamilnadu DR.M.G.R. Medical University in partial fulfillment of the M.D. Branch VIII Radio diagnosis Examination.

Director,
Barnard Institute of Radiology
Madras Medical College,
Government General Hospital,
Chennai.

ACKNOWLEDGEMENT

I would like to thank **Dr. P. MOHANASUNDARAM, MD, PhD**, Dean, Madras medical College, Chennai for giving me permission to conduct the study in this institution.

With extreme gratefulness, I express my indebtedness to **Prof. M. PRABAKARAN, MD, DMRD**, Director, Barnard Institute of Radiology, for having encouraged me to take up this study. But for his guiding spirit, perseverance and wisdom, this study would not have been possible.

I express my sincere thanks and gratitude to **Prof. T. S. SWAMINATHAN, M.D., D.M.R.D.,F.I.C.R.**, Former Director, Barnard Institute of Radiology for his immense kindness, constant support and consistent encouragement in conducting this study.

I am deeply indebted to my H.O.D, **Prof. N. KAILASANATHAN, M.D., D.M.R.D.**, whose help, stimulating suggestions and encouragement helped me in the research and writing of this thesis.

I wish to thank **Prof. K. MALATHY, M.D., D.M.R.D., Prof. A.P.ANNADURAI, M.D., D.M.R.D., Prof.K.VANITHA, M.D., D.M.R.D., D.R.M.,** and **Prof. K. THAYALAN** for their support, valuable criticisms and encouragement.

I am greatly indebted to my assistant professors **Dr.S.SUNDARESWARAN D.M.R.D., DR. NESAM MANIVANNAN, D.M.R.D., DR. S. KALPANA M.D., D.M.R.D., D.N.B., DR. S. BABU PETER, M.D., D.N.B., DR. D. RAMESH, M.D., DR. C. AMARNATH, M.D., D.N.B., F.R.C.R., Dr. J. DEVIMEENAL., M.D., D.M.R.D., D.N.B** and fellow postgraduates for their untiring help.

Last but not the least I thank all my patients for their cooperation, without whom this study would not have been possible.

CONTENTS

S.NO	TITLE	PAGE NO
1.	Introduction	1
2.	Aim of the study	3
3.	Review of literature	4
4.	Magnetization Transfer Imaging	13
5.	Tuberculoma	23
6.	Neurocysticercosis	33
7.	Materials and Methods	43
8.	Interpretation	47
9.	Results and Observation	49
10.	Discussion	55
11.	Conclusion	60
	Bibliography	
	Annexures Images	
	Proforma	
	Master chart	

Introduction

Single or multiple enhancing lesions in computerized tomography (CT) of brain may occur in several infectious and neoplastic diseases of the central nervous system and are the most common radiological abnormality seen in patients with acute-onset seizures in India and many other developing countries(1,2,3,6). Similar CT-documented lesions have also been reported in the developed world where these lesions are often considered to be caused by neoplasm or tuberculoma. (1)

Histopathological studies in India and even in some developed countries revealed that neurocysticercosis (NCC) is the most likely cause of these lesions. The second most common cause of these CT-detected lesions is tuberculoma; in patients with these lesions similar clinical and neuroimaging features are also present. Few authors believe that in poor and developing countries, where both tuberculosis and NCC are common, it is difficult to differentiate between tuberculoma and a single cysticercal granuloma.

The most interesting feature of these solitary enhancing lesions is their spontaneous disappearance within weeks or months. Some lesions "heal" by becoming calcified. These patients require only antiepileptic therapy, and this medication may be withdrawn safely after the lesion has resolved on CT scanning. In several studies provision of anticysticercal drugs has been attempted, but

because of conflicting results, their role in the management of these single lesions is uncertain. (1)

Using CECT and conventional MRI Brain, tuberculoma and neurocysticercus granuloma can be differentiated to some extent.(3) Various studies have shown that magnetization transfer ratio obtained using magnetization transfer MR imaging can differentiate tuberculoma from NCC.(8) This forms the basis of the study.

Aim of the study

To prospectively assess if Magnetization Transfer Ratio, obtained by using axial noncontrast Magnetization transfer imaging can help to differentiate Tuberculoma from Neurocysticercosis.

Review of literature

In Indian patients with acute onset seizures, solitary ring enhancing lesion is the most common imaging abnormality in contrast enhanced CT brain (1, 2, 3, 6). One of the points of controversy was whether these lesions were the cause or the effect of the associated seizure disorder. In 1980's ring enhancing lesions were presumed to be tuberculoma and treated with empirical Anti tubercular treatment.

A major break through came, when Chandy et al (1989), followed by Rajasekhar et al (1993) found on stereo tactic biopsy and histopathological studies that Neurocysticercosis is the commonest etiology of single enhancing lesion in CT scans. (3, 10)

Summary of causes of single enhancing lesions demonstrated on CT (1)

Common

NCC
Tuberculoma

In immunocompromised patients

Toxoplasmosis
CNS lymphoma
Fungal granuloma

Uncommon

Glioma
Secondaries
Cryptic AVM
Brain abscess
Larva migrans
Sarcoidosis
Small infarct
Focal encephalitis

Clinical presentation (1, 9, 14)

The patients in whom CT scanning reveals single enhancing lesions usually present with new-onset seizures. The seizures are often partial (motor / sensory) with or without secondary generalization. If a lesion is located in the occipital lobe, seizure is often preceded by visual aura, and in frontal lobe lesions an “adversive attack” is frequently observed. Cases of complex partial seizures are rare. Few patients present with partial status epilepticus several episodes of seizure occur in clusters, within a span of 2 to 3 days. Infrequently, Todd paralysis, which resolves within 24 hours, is observed. Another major complaint in patients with single enhancing lesions is headache.

Infections of the central nervous system (CNS) and single CT enhancing lesions (SCTEL) are the major provoking factors in patients with simple or complex partial seizure(s) with or without secondary generalization.(9).

Single computed tomography (CT) enhancing lesion (SCTEL) and focal cerebral calcification (FCC) accounted for 22% of the etiologic factors for localization-related epilepsies. The epilepsy associated with SCTEL was a form of benign epilepsy; epilepsy associated with FCC had remission rates similar to other remote symptomatic epilepsies. For this reason, we emphasize the need for neuroimaging

in patients with localization related epilepsies with unremarkable clinical findings, before classification into the cryptogenic category.

Differentiating cysticercus granuloma and Tuberculoma is difficult without resorting to an excision biopsy (1). Clinically, tuberculoma were associated with raised intracranial tension and focal neurological deficit. Tuberculoma are usually more than 20mm, are associated with midline shift, raised intracranial tension, and progression. (1, 3, 68). Basal meningitis with parenchymal lesions is highly suggestive of tuberculous etiology. Caseating tuberculoma with solid centre are hypo intense with hyper intense rim in T2 Weighted Images. (11, 12, 68)

Neurocysticercus granuloma are usually less than 20mm, no mass effect, no midline shift, no raised intracranial tension, and no progression. Cyst with dot inside (scolex) is diagnostic of Neurocysticercus granuloma. In Colloid vesicular stage, the cyst is hyper intense in T2WI. Degenerating cyst is hypo intense in T2WI when it mimics tuberculoma. (11,12). Advanced MRI techniques like Magnetization Transfer Imaging, Apparent Diffusion Coefficient and Magnetic Resonance Spectroscopy are used to differentiate the two lesions.

In 2001, Gupta R. K. et al. (13) conducted a study in six patients with intracranial tuberculomas. MT T1 and conventional spin echo MR imaging was performed and was compared with ex vivo MR imaging of the excised tuberculoma. The gross histopathology was compared with in vivo imaging with respect to the MR signal

intensity (MT ratio) in all six specimens. The MT outer hyperintense rim and hyperintense strands are due to the cellular infiltrate, noncaseating granulomas, and gliosis while the hypointense core represents solid caseation. The cellular outer rim shows lower MT ratio compared to the core of the tuberculoma. They concluded that histological correlation of the cellular and necrotic components of tuberculoma is best shown with MT T1 imaging.

In one other study, [Gupta RK](#) et al (33) concluded that when MT MR was used along with in vivo MR spectroscopy, it was possible to differentiate tuberculous brain abscesses from pyogenic brain abscesses, as both appear similar on conventional MR images. This differentiation would allow for better management of these cases.

In DWI, Vesicular and degenerating stages of cysticercus cysts from the core showed ADC values of $(1.66 \pm 0.29) \times 10^{-3}$ and $(1.51 \pm 0.23) \times 10^{-3} \text{mm}^2/\text{s}$, respectively, and were significantly higher than the core of all groups of tuberculomas and tuberculous abscess. So, addition of DWI to routine imaging protocol may help in differentiation of tuberculous lesions from degenerating cysticercus granuloma.

Recently, in vivo proton MR spectroscopy has been found to be helpful in better characterizing ring enhancing lesions; however, it may not always be possible to evaluate lesions smaller than 10 mm with in vivo spectroscopy owing to its

sensitivity constraints. Magnetization Resonance Spectroscopy can differentiate NCC and Tuberculoma. Tuberculoma / tuberculous abscess show prominent lipid, lactate but no amino acid residue. NCC show elevated lactate, alanine, succinate, and choline.

R.Gupta et al (35) have compared and analyzed the value of in vivo proton MR spectroscopy (PMRS) and T1 weighted magnetization transfer (MT) MR imaging in tissue characterization of brain tuberculomas. MT ratios from the rim and core of the tuberculomas were calculated and compared with metabolites seen on PMRS. They studied 33 cases of proven intracranial tuberculomas with in vivo PMRS and T1 weighted MT MR imaging. Spectroscopy showed only lipids at 0.9 ppm, 1.3 ppm, 2.0 ppm, and 2.80 ppm in 26 cases while lipids at 0.9 ppm, 1.3 ppm, 2.0 ppm and 2.80 ppm along with choline at 3.22 ppm was seen in remaining 7 patients. MT ratios from the core or solid necrosis varied from 21–29% while from the rim or cellular region varied from 16–24%. MT ratios from all the 33 lesions were consistent with tuberculomas while PMRS showed choline along with lipids in 7 predominantly cellular lesions simulating a neoplasm. They concluded that T1 weighted MT MR Imaging appears to be more consistent in the tissue characterization of brain tuberculoma.

In 1998, Kathuria MK et al (34) measured the magnetization transfer ratio (MTR) in different stages of neurocysticercosis. The visibility of a lesion on MT-SE

sequence was dependent on its MTR and its location at a particular site (cortical gray matter, white matter, or deep gray matter). The difference in MTR of the lesion and the surrounding brain parenchyma decides the resulting contrast and visibility of the lesion. Innocuous cystic lesions, which were hyperintense on T2-weighted images, did not show any MT (MTR = 5.10 ± 1.2), whereas degenerating T2 hyperintense lesions showed MTR of 26.40 ± 2.7 . Nondegenerating and degenerating scolices showed an intermediate MTR of 21.7 ± 3.3 and 15.0 ± 4.5 , respectively.

In 1998, Rakesh K. Gupta et al (8) studied 107 tuberculomas in seven patients with or without meningitis and fifteen patients with cysticercus granulomas with T2 hypo intensity. Five patients each with viral and pyogenic meningitis and two patients with cryptococcal meningitis were also studied. The MT ratios were calculated from tuberculomas, cysticercus granulomas, and thickened meninges in tuberculous, viral, pyogenic, and cryptococcal meningitis and were compared within each pathologic group and with the MT ratio of different regions of normal brain parenchyma. Detectability of lesions on T1-weighted MT spin-echo (SE) images was compared with that on conventional SE and post contrast MT-SE images. The tuberculous lesions with a hypo intense core on T2-weighted images had MT ratios of 23.8 ± 1.76 in the rim and 24.2 ± 3.1 in the core. There was no significant difference between the MT ratios in the core and the rim of these

lesions ($P > .5$). In the lesions that were isointense or invisible on SE images, MT ratios from the granulomas measured 26.04 ± 1.9 . T2 hyper intense lesions showed an MT ratio of 26.6 ± 1.94 . The MT ratio was significantly lower than that of white matter ($P < .001$) for all tuberculomas located in the sub cortical and deep white matter. The tuberculomas with a hypo intense core on T2-weighted images also showed a significantly lower MT ratio as compared with even the cortical gray matter ($P < .01$). However, the MT ratios of T2 hyperintense and invisible lesions were not significantly different from that of cortical gray matter ($P > .5$). The MT ratio from the 50 T2 hypointense cysticercus granulomas in 15 patients measured 32.1 ± 1.2 .

They concluded that Quantitative MT may differentiate T2 hypointense lesions of tuberculous origin from similar-appearing lesions of Neurocysticercosis.

In our study we have used Magnetization Transfer Imaging to calculate Magnetization Transfer Ratio of Tuberculoma and Neurocysticercosis and attempted to differentiate between the two lesions.

Constructive interference in steady state

This gradient echo sequence is a stimulated T2 echo. Two True FISP sequences are acquired with differing RF pulses and then combined for strong T2 Weighted high resolution 3D images. These True FISP sequences are normally affected by dark phase dispersion bands, which are caused by patient induced

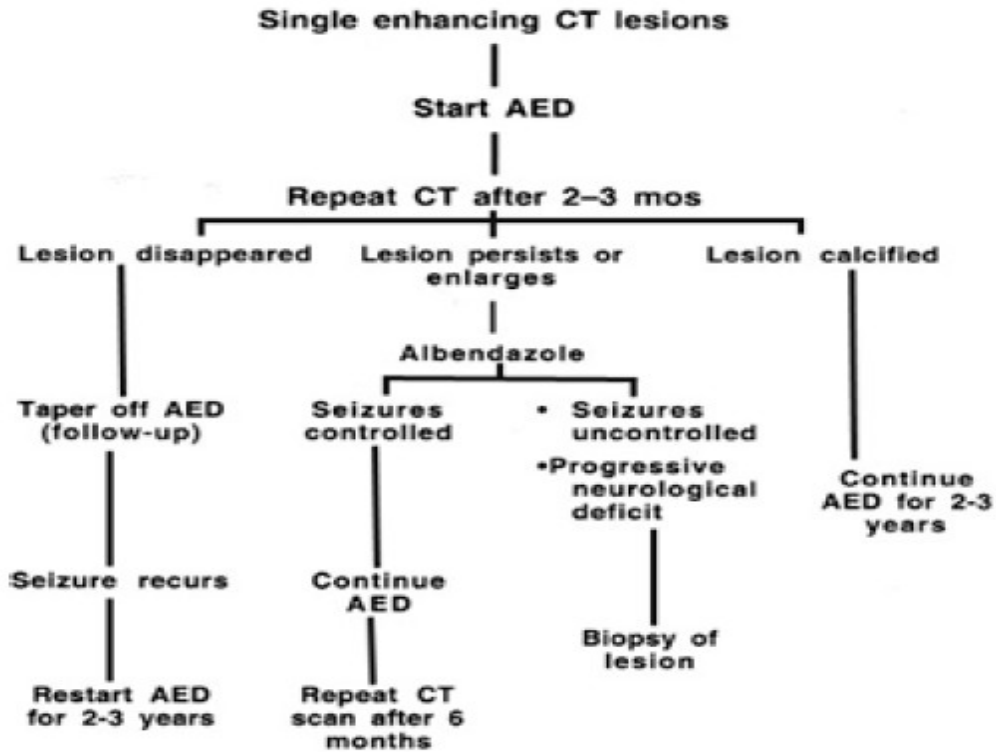
local field in homogeneities and made prominent by the relatively long TR used. The different excitation pulse regimes offset these bands in the 2 sequences. Combining the images, results in a picture, free of banding. The image combination is performed automatically after data collection, adding some time to the reconstruction process. The advantage of the 3D CISS sequence is its combination of high signal levels and extremely high spatial resolution.

Used for, e.g. inner ear, cranial nerves and cerebellum.

Srikanth Subbamma Govindappa et al (63) studied 11 patients with intraventricular cysticercal cysts. MR studies included spin-echo (SE) T1-weighted, turbo-SE T2-weighted, and 3D-CISS sequences. The routine sequences did not show the scolex, cystic wall, or cystic fluid together in any of the 11 patients. 3D-CISS images showed the scolex in all 11 patients and the cystic wall and cystic fluid in eight patients each. In seven of the 11 patients, 3D-CISS images showed the scolex, cystic wall, and fluid together.

The 3D-CISS sequence is more sensitive and specific than routine SE sequences in the diagnosis of intraventricular cysticercal cysts (60). So in our study we have included 3D CISS sequence to demonstrate scolex in neurocysticercosis.

Treatment algorithm for the management of patients with CT-documented single enhancing lesions.



AED = antiepileptic drug

Magnetization Transfer Imaging

Magnetization Transfer Imaging is a technique for improving image contrast in Magnetic Resonance (MR) imaging (16). It is based on application of off-resonance radio-frequency pulses and observing their effects on MR images. The magnetization transfer technique enables semi quantitative characterization of tissue and pathologic entities, which could substantially improve the specificity of MR imaging (16, 17, 18). By measuring the signal intensity with and without application of the pulses, magnetization transfer ratio (MTR) can be calculated. MTRs can be used to detect changes in the structural status of brain parenchyma that may or may not be visible with standard MR techniques.

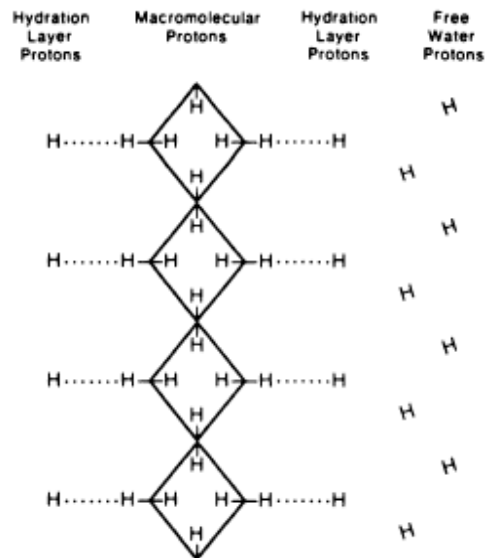
History

The employment of off-resonance irradiation was first proposed in an attempt to improve image contrast in 1983 by Muller et al (25). Wolff and Balaban (22) found that use of an off-resonance radio-frequency preparation pulse could generate excellent tissue contrast in images of rabbit kidney, and they referred to the technique as “Magnetization Transfer Contrast.” The utilization of magnetization transfer was extended to clinical imaging, including its use with gradient-echo imaging and MR angiography (21, 26, 27). It has also been used with short repetition time (TR) images to detect contrast enhancement and other regions containing short T1 elements, including methemoglobin (16) and lipid. It has been

proposed as the reason that adult white matter has high signal intensity on short TR images, even though it has 12% less water than gray matter (16).

In addition to being a new method of providing contrast, the magnetization transfer technique enables semi-quantitative characterization of tissue and pathologic entities, which could substantially improve the specificity of MR imaging (16,17).

Physical Mechanism

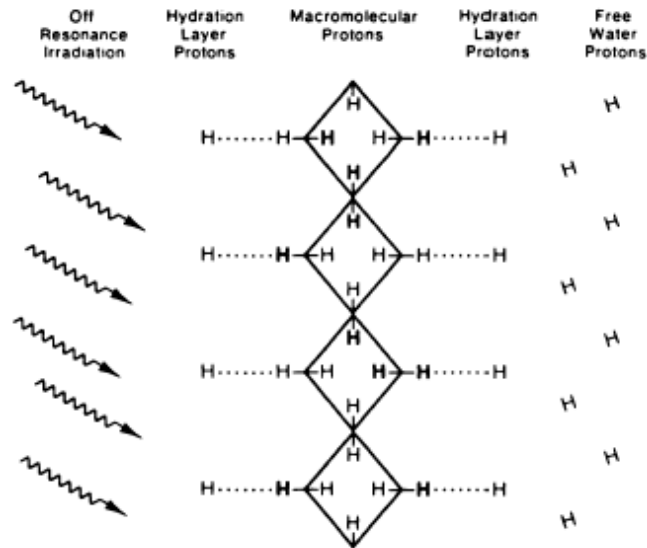


There are two pools of protons, free water protons and bound water protons. The signal obtained in clinical MR imaging comes from free water protons. There are, in addition, a large number of protons in tissues contained in macromolecules or in water bound to these macromolecules. No signal is normally detected from these protons by standard clinical imaging techniques because they have a very short T2 value (of the order of 1 ms or less) and any transverse magnetization is rapidly

dephased before data collection is possible. There is, however, a constant exchange of magnetization between the protons in these two pools, the free pool and the bound pool, which occurs by through-space dipole-dipole interactions or probably less importantly direct chemical exchange. By means of this interchange, the bound pool influences the signal obtained from the free pool even though the bound pool cannot be directly visualized.

In MT imaging, the normal equilibrium between free and bound pools is perturbed and the resulting contrast is referred to as magnetization transfer contrast and indicates the exchange processes with the bound pool in that particular tissue.

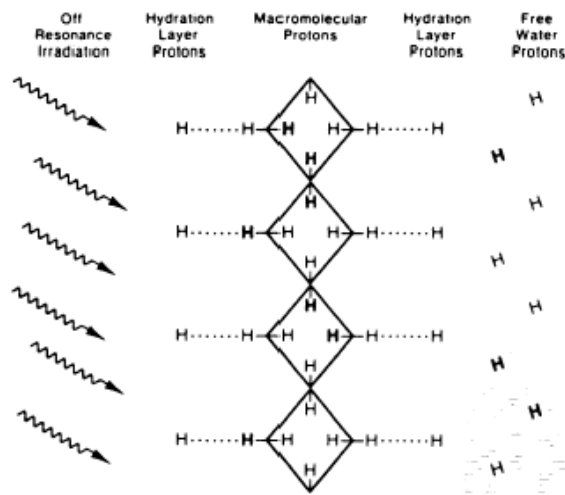
Wolff and Balaban(5) first produced in vivo images with MTC and described two-pool concept of magnetization transfer. They coined the terms free (H_f) and restricted (H_r) proton pools to describe the exchange compartments. These authors perturbed the normal equilibrium between free and bound pools by selectively saturating the bound pool.



Selective saturation: It is possible to saturate the macromolecular spins (i.e. to reduce their magnetization to zero) preferentially using radio frequency pulse. The restricted motion of protons results in a very short spin-spin relaxation rate (T_2). This results in a very broad absorption line shape (20-40 kHz) than the mobile spins (narrow water resonance peak of 15Hz), making them as much as 106 times more sensitive to an appropriately placed radio frequency pulse.

The saturated macromolecular spins, with zero magnetization will exchange for water spins having magnetization of one. Thus, when the magnetization of the water spins is subsequently measured, it will be found to be less than one.

The absolute reduction in magnetization will clearly depend, on the rate of exchange between the two spin populations, and hence can be detected with MR imaging.



MT Contrast (28): The reduction of magnetization in the water spins will be manifest as fewer signals, or less brightness on MR image, when compared to the "control" image obtained without the MT preparation. The decrease will be larger in regions where exchange of magnetization is more efficient, determined by the relative proportion of the hydrogen atoms of the two pools, their intrinsic relaxation times and the exchange rate.

Saturation transfer techniques (28): Three techniques for saturating the bound water have been studied: (a) off-resonance (radio frequency pulses applied at a frequency that is offset from the "free" water resonance) continuous wave excitation, (b) off-resonance shaped pulses, and (c) on-resonance binomial pulses. The off-resonance shaped pulses are now the commonest saturation transfer techniques for clinical imaging.

Magnetization transfer ratio (28): It is a quantitative measure of the MT effect on tissues. It is the degree of signal suppression of a given tissue compared with the conventional PD or T1-W image. The MT ratio (MTR) may be simply obtained by collecting a pair of identical images (PD or T1-W), one with and one without MT saturation. For each region of interest (ROI), MTR is calculated from the two images using the formula:

$$\text{MTR} = \frac{(M_0 - M_s)}{M_0} \times 100$$

Where M_0 , M_s represent the signal intensity with the saturation pulse off and on, respectively.

Factors affecting saturation transfer (28): There are several key parameters in the off-resonance saturation transfer technique that can alter the quantitative and qualitative MTR. The MTR measured depends upon the degree of saturation of the

bound water, and the degree of the direct saturation of the signal of the mobile protons and the exchange rate. The principle determinants being the base sequence used, characteristics of the saturating pulse (pulse type, power, duration, and time between pulses, duty cycle i.e. number of pulses per TR, bandwidth, and its effective flip angle), offset frequency of the saturating pulse, and field strength. All of these characteristics alter the degree of saturation obtained and must be known before quantitative comparisons can be made between clinical studies. Numerical values may be given, or the information displayed as a difference image.

Applications of MT imaging: (16, 17,28)

MTRs can be used to detect changes in the structural status of brain parenchyma that may or may not be visible with standard MR techniques. the magnetization transfer technique enables semi quantitative, reproducible characterization of tissue and pathologic entities, which could substantially improve the specificity of MR imaging.

In multiple sclerosis, lesions can be subcategorized into those with very low MTR (demyelinated lesions) and slightly decreased MTR (edematous lesions). In cases of wallerian degeneration, use of MTRs appears to allow reliable detection of changes undetectable with MR imaging or even light microscopy. In cases of infection with human immunodeficiency virus, MTRs seem to indicate that the macromolecular structure of white matter remains intact until relatively late in the

course of disease. In cases of metastasis, MTRs of brain lesions indicate structural changes beyond the extent of the lesions seen on standard MR images. These findings may be due to chronic edema, myelin loss, and perhaps previous undetected tumor.

MR Angiography: The use of an off-resonance saturation pulse with three-dimensional time-of-flight MR angiography increases the conspicuity of small arteries. Magnetization transfer contrast is now commonly used with time-of-flight angiography to increase vascular conspicuity.(21)

MT combined with paramagnetic contrast agents improves the detection of enhancing lesions, such as intracranial tumors, infection, and infarction (30)

In patients with active epilepsy who had a single calcified CT lesion, MT MR imaging can detect perilesional gliosis. Gliosis around a cerebral calcified lesion as seen on T1 weighted MT MRI indicates poor seizure control. (29).

MTR in Tuberculoma (8)

The T2 hypo intense Tuberculoma had the lowest MT ratios relative to T2 isointense / hyperintense Tuberculoma. Pathologically, the hyper intense and isointense (invisible) lesions are the solid granulomas with minimal or no caseation (5). With increased caseation, lesions tend to appear hypo intense on T2-weighted images. The caseation in a tuberculoma is composed predominantly of lipids and amino acids, as has been documented with proton MR spectroscopy (31). Lipids

are not known to show MT (32). The presence of lipids as the major macromolecular constituent of the caseating granulomas as compared with noncaseating granulomas is probably responsible for the lower MT ratios in the former. T2 hypo intense tuberculomas have shown much lower MT ratios as compared with gray and white matter, and are prominent on precontrast MT-SE images

MTR in Neurocysticercosis

T2 hypo intense cysticercus granulomas have a significantly higher MT ratio than do similar-appearing tuberculomas, and are of low visibility, especially when located in the white matter (8).

Quantitative MT ratios may help differentiate these similar-appearing infective granulomas and thus aid in the lesion-specific targeting of appropriate therapy. (8)

Tuberculoma

Involvement of the central nervous system occurs in 5 per cent of cases of tuberculosis, (11, 12, 37) and is especially common in patients younger than 20 years of age.

Tuberculosis is caused by *Mycobacterium tuberculosis* (TB), an acid-fast bacillus. It typically causes tuberculous meningitis (TBM) and/or localized CNS infection, tuberculoma. Most TB CNS infections are secondary result of hematogenous spread, often from pulmonary tuberculosis.

Meningitis is the most frequent manifestation of CNS TB and is more common in children. Childhood TB is typically a primary infection. Adult TB is most often post primary infection. Up to 30% occur due to primary infection. 10% of patients with tuberculomas also have TBM.

Pathogenesis: CNS TB almost always secondary to pulmonary TB; rarely Gastrointestinal or Genitourinary tract. Meningitis is caused by penetration of meningeal vessel walls by hematogenous spread or rupture of subependymal or subpial granulomata into the CSF. Tuberculoma is caused by hematogenous spread (GM-WM junction lesions) or by extension of meningitis into parenchyma via cortical veins or small penetrating arteries.

Arteries are directly involved by basilar exudates or indirectly by reactive arteritis (up to 40% of patients). Infection causes arterial spasm resulting in thrombosis and

infarct. Lenticulostriate arteries, MCA, thalamoperforators are most often affected. Infarcts are most common in basal ganglia, cerebral cortex, pons, and cerebellum. Arteritis is more common in children and HIV positive patients.

Clinical presentation (12): Varies from mild meningitis with no neurological deficit to comatose. Patients with TBM have fever, confusion, headache, lethargy and meningism. Patients with Tuberculoma have seizures, focal neurological deficits, increased intracranial pressure and papilledema.

Age: Occurs at all ages, more often in first 3 decades.

Gender: No gender predominance.

Laboratory investigations:

CSF analysis profile shows increased protein, pleocytosis (lymphocytes), and low glucose, negative for organisms. But CSF positive on initial LP in < 40%. Mycobacterium grows slowly; culture takes 4-8 weeks. PCR for TB may help confirm diagnosis earlier. TB skin test may be negative, particularly early. Elevated erythrocyte sedimentation rate common

The chest radiograph is abnormal in 45–60 per cent (37).

Clinical Features: (36)

Table 1: Multiple and solitary tuberculomas on presentation^[7-14]

Variables	Multiple tuberculomas	Solitary tuberculomas
Symptoms		
Meningeal irritation	++	+
Headache	++	++
Fever	++	+
Vertigo	+	+
Vomiting	++	+
Anorexia	+	+
Photophobia	+	+
Increased lethargy	++	++
Clinical signs		
Neck stiffness	++	+
Confusion	++	+
Coma	+	+
Cranial nerve III palsy	++	+
Cranial nerve VI palsy	++	+
Cranial nerve VII palsy	++	+
Hemiparesis	++	+
Seizures	+	++
CSF		
CSF glucose	-	-
Appearance clear	-	-
opening pressure	-	-
Total leucocyte count	-	-
Neutrophils	-	-
Lymphocyte	-	-
Protein	-	-
Lactate	-	-
Tuberculomas		
Ophthalmologic symptoms		29.5%
Intracranial hypertension		43.5%
Optic nerve atrophy		18.5%
Papillary oedema		43.7%
Hemiplegia		16.8%
Hemiparesis		30.5%
Monoplegia		10.5%
Aphasia		5.2%
Cerebellar syndromes		23.2%
Cranial nerves lesions		23.2%
Epilepsy		28.4%
Poor general state		9.5%
Pulmonary tuberculosis		12.6%
Lymph node tuberculosis		2.1%
Vertebral tuberculosis		6.3%
Tuberculin skin tests		70.3%
Anaemia		17.4%

++: More common; +: Less common; -: Slight changes or normal

Imaging findings:

Tuberculous meningitis is the most frequent manifestation and tends to involve the basal leptomeninges. CT shows obliteration of the basal cisterns by isodense or slightly hyper dense exudates, which shows diffuse enhancement with IV contrast medium. The most useful CT criteria of abnormal basal meningeal enhancement are: (A) linear enhancement of the middle cerebral artery cisterns; (B) obliteration by contrast of the CSF spaces around normal vascular enhancement; (C) Y-shaped enhancement at the junction of the suprasellar and middle cerebral artery cisterns and (D) asymmetry of enhancement (37). The meningeal exudates obstruct CSF resorption and causes communicating hydrocephalus; this is seen in 50 per cent of adults and 85 per cent of children (37).

Meninges were visible on pre-contrast T1 weighted MT images only in patients with tuberculous meningitis(Fig 2).The MTR from meninges in tuberculous infection was 19.10 ± 1.02 , and the percentage difference in the mean SI of the meninges and the adjacent T2 normal brain parenchyma was significantly higher ($p < 0.05$) in the tuberculous group compared with that in the nontuberculous group. MT MRI is an important technique for the detection and characterization of infectious meningitis of different etiology. Visibility of the meninges on pre-contrast T1 weighted MT images may be considered highly suggestive of

tuberculous meningitis. (38) In TBM, there is marked meningeal enhancement, basilar prominence; may be nodular meningeal enhancement

Infarctions of the basal ganglia and internal capsules can occur, caused by an arteritis of the penetrating arteries at the base of the brain

Tuberculomas are typically parenchymal, mainly supratentorial (often parietal lobes) (37). Infratentorial lesions are less common, can involve brainstem (up to 8%). Dural tuberculomas may occur. In one Study (39) of 100 consecutive tuberculoma, multiple tuberculomas and infratentorial locations were more common (in the authors' patient population than in previous reports). They range in size from 1 mm to 6 cm.

Parenchymal granulomas occur most often at the corticomedullary junction. 10% of patients with tuberculomas also have TBM. Solitary or multiple (more common).

On CT, they appear as small, rounded lesions isodense or hypo dense to brain, with variable amounts of surrounding edema. Enhancement is homogeneous when lesions are solid (Fig 3) and shows rim enhancement when central caseation or liquefaction occurs. The 'target sign' of central high attenuation with rim enhancement is not pathognomonic for tuberculoma.

On MRI, small tuberculomas show prolonged T1 and T2; caseation results in low signal on T2W images. Tuberculomas may calcify when healed, but, as with meningeal disease, this is uncommon.

Tae Kyoung Kim et al (44) have compared MR findings of tuberculoma with histopathology. On T1-weighted images, histologic correlation revealed that the central isointensity or mixed isointensity and hyperintensity corresponded to caseation necrosis with adjacent inflammatory cellular infiltrates. Surrounding slight hyperintense and hypointense rims corresponded to a layer of collagenous fibrosis and a layer of outer inflammatory cellular infiltrates, respectively. The hyperintensity of the fibrotic layer may be related to the relatively high protein concentration and low water content compared with adjacent tissue.

Wasay M et al in their study of Brain CT and MRI findings in 100 consecutive patients with intracranial tuberculoma (52) stated that MRI signal characteristics of intracranial tuberculoma are extremely diverse. An iso intense or hypo intense core with a hyper intense rim on T2-weighted and FLAIR images is the most common presentation.

Gupta RK has quoted in a study that granulomas showing more macrophages, fibrosis and gliosis appeared hypo intense on T2-weighted images while tuberculomas showing minimal macrophages, marked cellular infiltration, and minimal fibrosis appeared hyper intense on T2-weighted images. In addition, hypo

intense lesions showed marked increase in peaks in the region of mobile lipids (1.28 ppm) compared to normal brain parenchyma in localized proton spectroscopy. (42)

Tuberculous abscesses are uncommon; they may resemble tuberculomas but are usually larger with a thinner enhancing rim (37).

Tuberculoma can be Noncaseating, caseating with solid center, or caseating with necrotic center. They rarely progress to TB abscess

Noncaseating tuberculoma: Hypo intense to brain in T1WI, hyper intense to brain in T2WI and FLAIR and show nodular, homogeneous enhancements in contrast study.

Caseating granuloma with solid center: Hypo intense or isointense to brain in T1WI, iso- to hypo intense with hypo intense rim (hypo intensity due to free radicals, solid caseation or increased cellular density) in T2WI. On contrast, Nodular, homogeneous enhancement

Caseating granuloma with necrotic center: Hypo intense or isointense to brain with central hypo intensity in T1WI, central hyper intensity with hypo intense rim with surrounding edema common in T2WI. On contrast, there is peripheral rim enhancement and central low signal.

On T1-W MT imaging, T2 hypointense tuberculoma has a hypointense core and a hyperintense rim. (Fig 1). On histopathology, the T2 and MT hypointense central

core matched with the solid caseation while the MT hyperintense rim (usually not seen on T2-W images as it merges with surrounding edema) showed variable amounts of cellular infiltrate, granulomas, Langhan's giant cells and gliosis/fibrosis. Mycobacterium tuberculosis is rich in lipids and produces fewer proteins and amino acids. The MT ratio is influenced by the concentration of proteins and amino acids. Fewer the proteins and amino acids, lower is the MT Ratio in Tuberculoma.

It may also be possible to differentiate T2 hypointense tuberculoma from T2 hypointense cysticercus granuloma with the use of MTR, as cysticercus granuloma shows significantly higher MT ratio compared to tuberculoma.

[Gupta RK](#) et al (13) in a study have concluded that the histological correlation of the cellular and necrotic components of tuberculomas is best shown with MT T1 imaging. The MT hyper intense rim matched the cellular component of the tuberculoma that was masked on T2-weighted images because of the associated perifocal edema. The cellular component had a lower MT ratio compared to the necrotic components.

M. K. Vasudev et al (40) evaluated thirty-three patients with intracranial tuberculomas (histologically confirmed in 22) with proton density/T2-weighted, T1-weighted (with and without MT), and echo-planar diffusion-weighted imaging sequences. T2 relaxation times, MT ratios (MTR), and apparent diffusion

coefficient (ADC) values were calculated from the center of the lesion, the periphery, perilesional edema, and contra lateral normal white matter. The measured mean values of T2 relaxation time, MTR, and ADC in the center of lesions were 155.5 ms, 14.1, and 1.27×10^{-3} mm²/s, respectively, compared to 117 ms, 23.72, and 0.74×10^{-3} mm²/s in normal white matter, and a T2 relaxation time of 187.45 ms in normal gray matter. They concluded that intracranial tuberculomas are characterized by relatively short T2 relaxation times (compared to normal gray matter), decreased MTR, and mostly no restriction of diffusion. A combination of these quantitative parameters could be of help in the noninvasive diagnosis of tuberculomas.

Rare: Ventriculitis, choroid plexitis, pachymeningitis with dural thickening and enhancement (may mimic meningioma)

MRA: May see vessel narrowing, irregularity, occlusion

MRS in TB abscess has prominent lipid, lactate but no amino acid resonances,

Lipids at 0.9 ppm, 1.3 ppm, 2.0 ppm, 2.8 ppm

Complications: Hydrocephalus, ischemia common

Chronic changes: Atrophy, Ca⁺⁺, chronic ischemia.

Angiographic Findings

Conventional - Narrowing of major arteries at base of brain (supraclinoid ICA, MCA, ACA)

Narrowing and occlusion of small and/or medium sized arteries

Abnormal blush, early venous drainage

Imaging Recommendations

Best imaging tool: MRI is most sensitive to delineate extent and complications

Protocol advice: Contrast-enhanced MRI with FLAIR, DWI, +/- MRA

Natural History & Prognosis

Long term morbidity is up to 80% which includes Mental retardation, paralysis, seizures, rigidity, speech or visual deficits. Mortality is 25-30% of patients; higher in AIDS. Complications: Hydrocephalus (70%), stroke (up to 40%), cranial neuropathies (3, 4, 6 common), syrinx. Tuberculomas may take months to years to resolve. Size of lesion determines healing time.

Treatment: Untreated TBM can be fatal in 4-8 weeks. Multidrug therapy is given. Isoniazid, rifampin, pyrazinamide, +/- ethambutol or streptomycin. Despite therapy, lesions may develop or increase. Hydrocephalus typically requires CSF diversion.

TB mimics other diseases like neoplasm, hence follow up imaging is done. Giant extra-axial tuberculoma can masquerade as meningioma. (45,46, 47).

Neurocysticercosis

Neurocysticercosis (NCC) remains a major public health problem in developing and some developed countries (48). Neurocysticercosis is now recognized as a common cause of neurological disease in developing countries and the United States (49). NCC is the cause of nearly one-third of all cases of AE in both the urban and rural regions in south India (51).

Taeniosis and cysticercosis, diseases caused by the parasitic tapeworm *Taenia solium*, are distributed worldwide where pigs are eaten and sanitation is poor, and also in the more developed countries as a result of increasing migration (50). The disease Taeniasis or pork tapeworm infection results from infestation of the small intestine by *Taenia solium*, the adult tapeworm. Humans are both the definitive and intermediate hosts for *Taenia solium*. Cysticercosis is a disease caused by the presence of *Cysticercus cellulosae* and *Cysticercus racemose*, the larval forms of *Taenia solium* in tissues. The infection occurs from contamination of food (usually vegetables) with viable eggs from human excreta, from fecal-oral contact or from auto-infection due to reverse peristalsis of proglottids in to the stomach. The embryos most commonly mature in the brain, skeletal muscle and eye. (52)

Cysticerci are ovoid cysts that contain an invaginated larval head, or scolex.

The less virulent form, *Cysticercus cellulosae*, is a small (< 2 cm), thin-walled round cyst that lodges in the parenchyma or subarachnoid space and provokes only a minor inflammation. Consequently, these cysts often remain silent. On the other

hand, the larger, more virulent and intense form, *Cysticercus racemose*, grows actively to form grape-like clusters of cysts in the basal cisterns and ventricles. *Cysticercus cellulosae* has a predilection for the dorsolateral subarachnoid space, while the *Cysticercus racemose* has a predilection for the basal subarachnoid cisterns. (52)

Four pathologic stages: Vesicular, colloidal vesicular, granular nodular, nodular calcified

Cysticerci are seen most commonly in the convexity subarachnoid spaces. May involve cisterns > parenchyma > ventricles. Parenchyma cysts are often hemispheric, at the gray-white junction. Intraventricular cysts are often isolated. Fourth ventricle is the most common location. Basal cistern cysts may be racemose (grape-like). Subarachnoid cysticerci, which usually lack a scolex, may cause obstructive hydrocephalus. Rare CNS locations: Sella, orbit, spinal cord.

Cysts variable, typically 1 cm, range from 5-20 mm.

Neurocysticercosis has varied imaging appearances depending on the developmental stage of the larva. In the vesicular stage the parasite is alive and incites little or no perilesional oedema. The cyst is isointense to CSF, the scolex isointense to white matter. Enhancement is minimal or absent. In the colloidal vesicular stage the larva dies and lesions show ring enhancement with surrounding

edema. Cyst retraction in the granular nodular stage results in small enhancing nodules with mild edema. Finally, in the nodular calcified stage, the lesions calcify.

Clinical Manifestations

The disease may remain asymptomatic. Seizures are the most common symptom occurring in 70-90% of patients having brain parenchymal cyst or calcification. Seizures are often generalized tonic-clonic, simple partial or complex partial type. A well-known complication of neurocysticercosis is cerebral arteritis, which is usually manifested by cerebral ischemia. Mostly these are in the form of an endarteritis involving the smaller basal vessels due to basal exudates. When cysticerci lodge within the ventricular system, life-threatening acute intracranial hypertension secondary to hydrocephalus may develop. Cysts in the Subarachnoid space may invade the Sylvian fissure and grow to large sizes (giant cysts) causing intracranial hypertension with hemiparesis, partial seizures or other focal neurological signs.

Clinical manifestations are nonspecific, most neuroimaging findings are not pathognomonic, and some serologic tests have low sensitivity and specificity.

The clinico-radiological criteria proposed by Rajshekhar (1991) are valid and reliable in predicting a benign outcome. CT follow-up within the first 4 weeks is critical. **(3,10)**

Clinical : seizure (partial or generalized) as initial symptom, no persistent raised ICP, no progressive neurological deficit, no active systemic disease. CT Brain: solitary, contrast-enhancing lesion, 20-mm diameter lesion, no severe cerebral edema (no midline shift).

Proposed diagnostic criteria for Neurocysticercosis by O. H. Del Brutto, MD et al provide diagnostic criteria for Neurocysticercosis based on objective clinical, imaging, immunologic, and epidemiologic data. (53,54)

Absolute

Histological demonstration of the parasite
Cystic lesions showing the scolex
Direct visualization of sub-retinal parasites

Major

Lesions highly suggestive of neurocysticercosis like cystic lesions without scolex, enhancing lesions, or parenchymal calcifications
Positive serum EITB
Resolution of intracranial cystic lesions after therapy
Spontaneous resolution of small single enhancing lesions

Minor

Lesions compatible with neurocysticercosis like hydrocephalus
Clinical manifestations suggestive of neurocysticercosis like Seizures.
Positive CSF ELISA
Cysticercosis outside the CNS

Epidemiological

Evidence of a household contact
Individuals coming from or living in an area where cysticercosis is endemic
Frequent travel to disease-endemic area

Definitive diagnosis: Presence of one absolute criterion; Presence of two major plus one minor and one epidemiological criterion.

Probable diagnosis: Presence of one major plus two minor criteria; Presence of one major plus one minor and one epidemiological criteria; Presence of three minor plus one epidemiological criteria

Revised diagnostic criteria for neurocysticercosis (53,55)

Absolute

Histological demonstration of the parasite

Multiple cystic lesions with or without scolex on CT or MRI

Major

Lesions highly suggestive of neurocysticercosis like cystic lesions without scolex, enhancing lesions, or parenchymal calcifications

Spontaneous resolution or eventual calcification of the lesion

Positive serum EITB assay for the detection of antibodies against the parasite

Minor

Presence of a characteristic clinical picture

Positive CSF ELISA

Cysticercosis outside the CNS

Aggravation of existing symptoms or appearance of a new symptom following anticysticercal therapy

Diagnosis with caution in the presence of certain conditions*

Old age

Patients with pre-existing systemic tuberculosis or malignancy

Presence of HIV infection

Grossly abnormal neurological examination.

Definitive diagnosis: Presence of one absolute criteria; Presence of two major plus one minor

Probable diagnosis: Presence of one major plus two minor criteria; Presence; Presence of three minor

Serological Tests

Currently, the best procedures for diagnosing NCC are neuroimaging studies.

Immunoserologic assays, such as enzyme-linked immunoelectrotransfer blot assay (EITB) or enzyme-linked immunosorbent assay (ELISA), detect antibodies against

Taenia solium, or *cysticercus*. Consequently, they are useful in identifying a population at risk of contact with the parasite but do not necessarily indicate a

systemic active infection(48). Immunological assays detect positivity for human cysticercosis in 8—12% of people in some endemic regions, which indicates the presence of antibodies against the parasite but not necessarily active or central-nervous-system infection (57). Most seropositive individuals are asymptomatic. No data from prospective studies concern the proportion of these individuals that will develop seizures or other neurologic symptoms. The gold standard serodiagnostic assay for cysticercosis and neurocysticercosis, diseases caused by the metacestode of *Taenia solium*, uses lentil lectin-purified glycoprotein (LLGP) in a Western blot assay (56)

Imaging Findings

There is a discrepancy between the results of serologic assays and neuro imaging studies: >50% of those individuals with neurocysticercosis diagnosed by computed tomography (CT) scan test EITB negative (48). The only reliable tool for diagnosis of neurocysticercosis is imaging by CT or MRI (57).

HR Martinez et al studied the MR findings in 56 patients with neurocysticercosis (NCC) and concluded that MR is sensitive in the diagnosis of active NCC and may be useful in evaluating the degenerative changes in the parasite that occur as a result of natural degeneration, host response, or medical therapy (58).

Rajshekhar and Chandy (in a large series of patients) demonstrated that for Indian patients with seizures and spontaneously resolving small single enhancing lesions,

the diagnosis of neurocysticercosis could be accomplished with a 99.5% sensitivity and a 98.9% specificity(59).

Vesicular stage (viable larva):

NECT Smooth, thin-walled cyst, isodense to CSF, no edema

Hyper dense "dot" within cyst = proto scolex

CECT Vesicular stage: No (or mild) wall enhancement

MRI cystic lesion isointense to CSF with a discrete, eccentric scolex and no surrounding edema.

Typically no or mild enhancement is seen.

Colloidal vesicular stage (degenerating larva):

NECT Hyper dense cyst fluid with surrounding edema

CECT Thicker ring-enhancing fibrous capsule

MRI Cyst is mildly hyperintense to CSF in all sequences.mild to marked surrounding edema. Thick cyst wall enhances, with an enhancing marginal nodule (scolex)

Granular nodular (healing) stage:

NECT Mild edema

CECT Involuting enhancing nodule

MRI Thickened, retracted cyst wall; edema decreases
may have nodular or ring-enhancement

Nodular calcified (healed) stage:

NECT Small, Ca⁺⁺ nodule

CECT Shrunken, calcified nodule

MRI Shrunken, Ca⁺⁺ lesion rare
minimal enhancement

"Encephalitic cysticercosis" with multiple small enhancing lesions and diffuse edema are seen in children. Intraventricular cysts may cause ventriculitis and/or hydrocephalus. Better Seen In FLAIR images. Cisternal NCC may appear racemose (multilobulated, grape-like), typically lacks scolex.

T1-W MT imaging improved lesion detectability and the lesions that were "CSE invisible" were detected. These lesions appeared as central hypointense core with peripheral hyperintensity.

T1-W MT images are also important in demonstrating perilesional gliosis in treated neurocysticercus lesions. On MRI, gliosis is observed in a small number of patients with epilepsy and appears as hyperintense on T2-W images. T1-W MT imaging improves detection of perilesional gliosis not visible on CSE MR imaging, and is seen as hyperintensity around the lesion. Gliotic areas show low MTR compared to the gray matter and white matter. The patients with gliosis may have seizures that could be difficult to control with a single anti-epileptic drug and may

have a higher incidence of seizure recurrence after withdrawing anti-epileptic drug therapy.

MR Spectroscopy: Few reports show elevated lactate, alanine, succinate, choline; decreased NAA and Creatinine.

The 3D-CISS sequence is more sensitive and specific than routine SE sequences in the diagnosis of intraventricular cysticercal cysts (60).

DWI: Cystic lesion typically isointense to CSF

Complications: Meningitis, hydrocephalus, vasculitis

Treatment should be individually fitted for each patient, with antiepileptic drugs, analgesics, corticosteroids, or a combination of these. Anthelmintic drugs (praziquantel and albendazole) are used routinely, but so far no controlled clinical trial has established specific indications or definitive doses of treatment. In patients presenting with seizures due to single viable parenchymal neurocysticercosis, albendazole hastens the resolution of SSECTL if treatment is given in the early phase of the illness(31)

Parenchymal forms of neurocysticercosis have a good prognosis in terms of clinical remission. The most effective approach to taeniosis and cysticercosis is prevention, which should be a primary public-health focus for less developed countries (28).

Treatment outcome: Vedantam Rajshekhar, MCh and Lakshmanan Jeyaseelan, PhD et al prospectively studied 185 patients with SCCG and seizures in whom AEDs were withdrawn soon after (within 2 to 12 weeks) resolution of the SCCG was demonstrated on the CT scan. The follow-up of these patients ranged from 24 to 125 months (mean 65.8 months) or until seizure recurrence. Age, number of seizures, duration of AED therapy, occurrence of breakthrough seizures, administration of albendazole, and presence of a calcific residue of the SCCG on the CT scan were studied as prognostic factors to predict recurrence of seizures.

Nearly 85% of patients with a solitary cerebral cysticercus granuloma have a good seizure outcome following resolution of the lesion and early withdrawal of Antiepileptic Drugs. However, recurrence of seizures can be expected in about 15% of patients. Patients with more than two seizures, those with breakthrough seizures, and those whose follow-up CT scan shows a calcific residue of the granuloma have a higher risk of recurrence and therefore need to be appropriately cautioned after withdrawal of AEDs.(62).

Neurocysticercosis is a potentially eradicable disease but this is probably unlikely to be achieved in the short term (61).

Materials and Methods

The study was performed in 1.5 Tesla SIEMENS MAGNETOM SYMPHONY, a superconductive MRI scanner.

Study place: Barnard Institute of Radiology, Madras Medical College, Chennai.

Study period: Nov 2008 – Oct 2009.

Inclusion criteria: patients clinically suspected of having intracranial granuloma, who had ring enhancing lesions in Contrast Enhanced Computed Tomography (CECT) or Magnetization Resonance Imaging of Brain.

Exclusion criteria:

1. All patients with calcified granuloma.
2. Patients with known primary malignancy.
3. Patients with claustrophobia.
4. Patients with other contraindications –pacemaker implants, cochlear

implants etc.

Data collection

All patients provided the informed consent for performing additional sequences during imaging. Brief history regarding the nature and duration of illness, treatment history, significant past and personal history is taken from all patients.

Methods

All patients were examined with MRI Brain.

Sequences used:

Conventional spin echo T1-Weighted (TR 1000, TE 14) non contrast
axial MR images without off - resonance saturation pulse.

Conventional spin echo T1-Weighted (TR 1000, TE 14) non contrast
axial MR images with an off - resonance saturation pulse.

Ps3d / 3d CISS sequence

The off - resonance saturation pulse was obtained immediately before the 90° excitation pulse to saturate the magnetization of protons with restricted motion. All images were obtained in axial plane with 5mm slice thickness and a base resolution of 192 x 256 matrixes.

Ps3d / 3d CISS sequence was obtained for the demonstration of scolex in all patients.

Images were analyzed by two separate radiologists. Signal intensity from the region of interest (rim of the granuloma) was obtained with a single pixel from the conventional T1WI (without an off resonance pulse) and MT images (with an off resonance pulse).

For each region of interest (ROI), MTR is calculated from the two images using the formula:

$$MTR = \frac{(M_o - M_t)}{M_o} \times 100$$

Where, M_o - the signal intensity with saturation pulse off
 M_t - the signal intensity with saturation pulse on, respectively.

Consistency and reliability of the measurements were confirmed by obtaining the values repeatedly.

The final diagnosis of tuberculosis was based on typical CSF features (cellularity and biochemistry), histopathological examination and response to specific treatment. The diagnosis of Neurocysticercosis was based on the presence of scolex in a cyst in ps3d/ 3d CISS sequence in MR Images. As per the Revised diagnostic criteria for Neurocysticercosis , the presence of multiple cystic lesions with or without scolex on CT or MRI is an Absolute criterion for the definitive diagnosis of neurocysticercosis.

Statistics:

The lesions were grouped as Tuberculoma, cystic NCC (T2 hyper intense, follows CSF intensity) and degenerative NCC (T2 hypointense / hyperintense). The MT Ratio obtained from the rim of the lesion was tabulated and analyzed using ANOVA method. The Mean MT ratios were obtained for each category with Standard Deviation from the Mean.

The final diagnosis of tuberculosis was based on typical CSF features (cellularity and biochemistry), histopathological examination and response to specific treatment. The diagnosis of Neurocysticercosis was based on the presence of scolex in a cyst in ps3d/ ciss sequence in MR Images. As per the revised diagnostic criteria for neurocysticercosis, presence of multiple cystic lesions with or without

scolex on CT or MRI is an Absolute criterion for the definitive diagnosis of neurocysticercosis.

Interpretation

The number, location and signal intensity of the granuloma in T1 and T2 Weighted images was noted.

The presence of scolex within a cystic lesion was noted in ps3d / 3d CISS images.

Signal intensity from the Region of Interest was measured from conventional T1 WI and MT images. The ROIs were obtained with a single pixel in the rim of the lesion. Mo and Mt values were obtained repeatedly to maintain consistency and reliability of the measurement.

For each region of interest (ROI), MTR is calculated from the two images using the formula:

$$MTR = \frac{(M_o - M_t)}{M_o} \times 100$$

Where, M_o . the signal intensity with saturation pulse off

M_t . the signal intensity with saturation pulse on, respectively.

Presence of additional findings like infarct, meningeal thickening, basal meningitis was noted.

The MT Ratio from the cortical and deep gray and white matter was also obtained.

It includes Frontal, parietal, occipital and temporal regions, head of caudate nucleus and thalamus. (Fig 6)

Lesions were grouped as Tuberculoma, cystic Neurocysticercosis and degenerating Neurocysticercosis. Cystic lesions isointense to CSF in all sequences were considered as innocuous cystic Neurocysticercosis. Cystic lesions mildly hyperintense to CSF in all sequence with thickened retracted wall or shrunken were considered degenerating Neurocysticercosis.

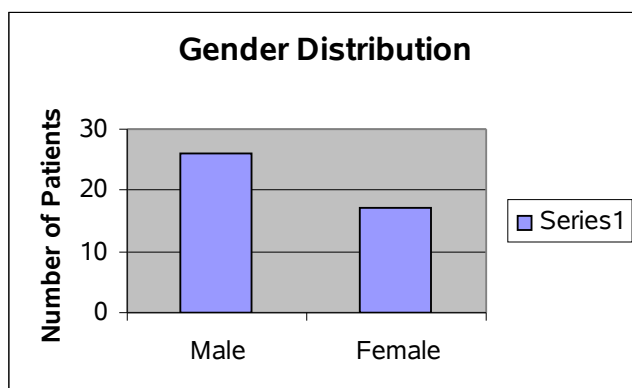
The MTR were tabulated for each group and compared using ANOVA method of statistical analysis. The Mean MTR was obtained for each group.

Results and observation

The study group consists of 43 patients suspected of having intracranial granuloma.. They had ring enhancing lesions in CECT or MRI Brain. A total of 76 granulomas were analyzed

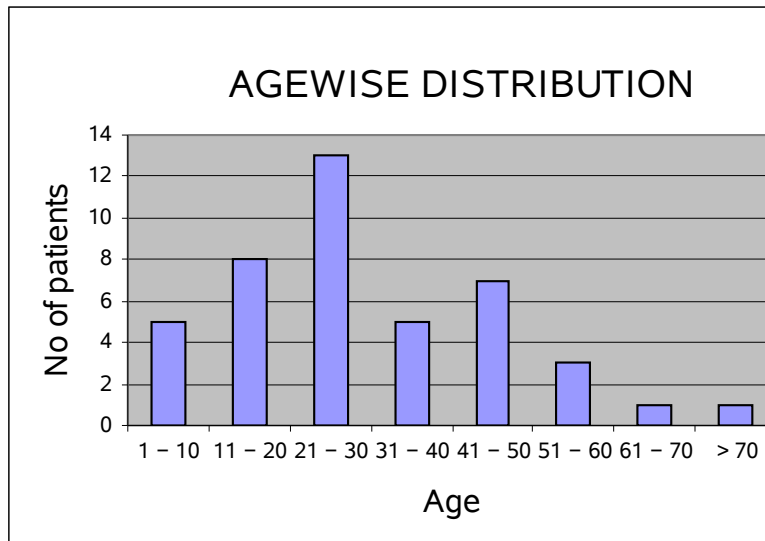
Gender distribution

26 patients were men and 17 patients were women.



Age distribution

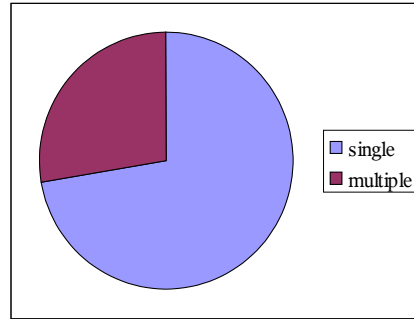
Age ranged from 6 to 72 years.



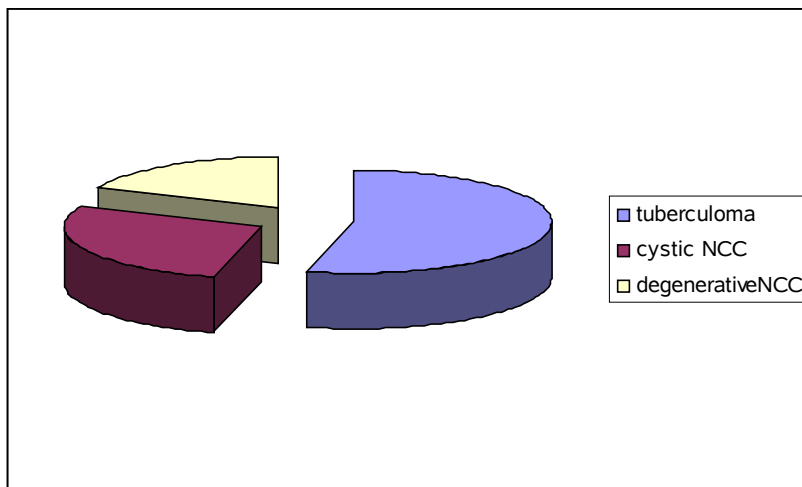
21 patients had intracranial tuberculoma. 22 patients had Neurocysticercosis. The final diagnosis of tuberculosis was based on typical CSF features (cellularity and biochemistry), histopathological examination and response to specific treatment. Histopathological evidence of tuberculosis was present in one patient with Tuberculous abscess in the left middle cerebellar peduncle. The typical radiological features of miliary pulmonary tuberculosis were present in 4 patients. The diagnosis of Neurocysticercosis was based on the presence of scolex in a cyst in ps3d/ ciss sequence in MR Images.

The MT Ratio of the normal white matter and deep gray matter from healthy controls measured 23.72 ± 2.36 and 17.58 ± 3.52 respectively. The data was taken for comparison with tuberculomas and T2 hypointense cysticercus granulomas.

31 patients had single ring enhancing lesion. Multiple ring enhancing lesions were seen in 12 patients.



A total of 76 granuloma were analyzed. Of which, 41 were tuberculoma and 35 were Neurocysticercus. 41 Tuberculomas in 21 patients were analyzed. 35 Neurocysticercus lesions were analyzed in 22 patients. Cystic vesicular Neurocysticercus was 21 and degenerating Neurocysticercus was 14.



Mean MTR for tuberculoma is 16.6 ± 3.1 (15.6 –17.56). One patient had Tubercular abscess which was present in the left Middle cerebellar peduncle which was having T2 hyperintense core which showed diffusion restriction. MT Ratio

from the rim of the abscess was 10.7 – 12, which was significantly lower than that of surrounding brain parenchyma.

Descriptives

MTR

	N	Mean	Std. Deviation	Std. Error	95% Confidence Interval for Mean		Minimum	Maximum
					Lower Bound	Upper Bound		
NCC - VESICULAR	21	10.9000	2.82981	.61752	9.6119	12.1881	2.90	14.70
NCC - DEGENERATING	14	20.8500	3.57378	.95513	18.7866	22.9134	16.70	28.00
TUBERCULOMA	41	16.5944	3.08239	.48139	15.6215	17.5673	6.00	22.10
Total	76	15.8049	4.60920	.52871	14.7516	16.8581	2.90	28.00

ANOVA

MTR

	Sum of Squares	df	Mean Square	F	Sig.
Between Groups	887.116	2	443.558	45.848	.000
Within Groups	706.236	73	9.674		
Total	1593.353	75			

There were 21 innocuous cystic lesions (representing vesicular stage of NCC) which showed mean MTR of 10.9 ± 2.8 (9.6 – 12.18). There were 3 lesions which were hypointense on T2WI which showed a mean MTR which was significantly higher (23.725 ± 3). 14 lesions with imaging features suggestive of degenerative cysts showed MTR of 20.8 ± 3.5 (18.7 – 22.9).

Post Hoc Tests

When multiple comparisons are made, the mean difference between the ratio of the three groups is significant.

Multiple Comparisons

Dependent Variable: MTR

Tukey HSD

(I) DIAGNOSIS	(J) DIAGNOSIS	Mean Difference (I-J)	Std. Error	Sig.	95% Confidence Interval	
					Lower Bound	Upper Bound
NCC - VESICULAR	NCC - DEGENERATING	-9.9500*	1.07318	.000	-12.5175	-7.3825
	TUBERCULOMA	-5.69439*	.83466	.000	-7.6913	-3.6975
NCC - DEGENERATING	NCC - VESICULAR	9.95000*	1.07318	.000	7.3825	12.5175
	TUBERCULOMA	4.25561*	.96281	.000	1.9522	6.5591
TUBERCULOMA	NCC - VESICULAR	5.69439*	.83466	.000	3.6975	7.6913
	NCC - DEGENERATING	-4.25561*	.96281	.000	-6.5591	-1.9522

*. The mean difference is significant at the .05 level.

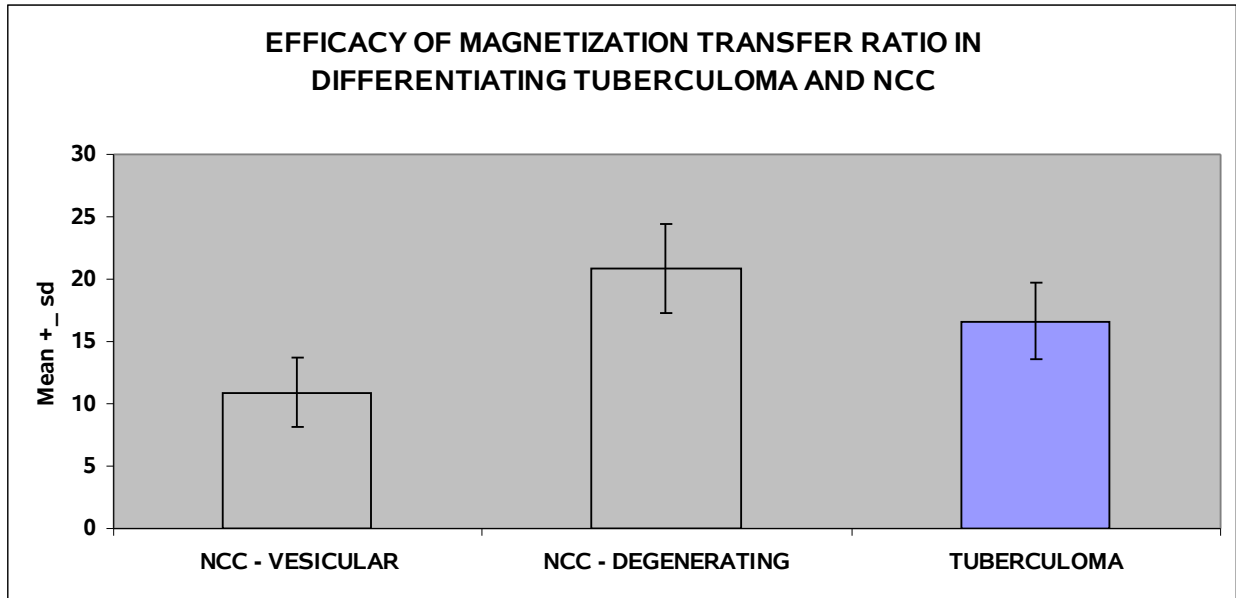
T-Test

Group Statistics

DIAGNOSIS		N	Mean	Std. Deviation	Std. Error Mean
MTR	NCC	35	14.8800	5.83552	.98638
	TUBERCULOMA	41	16.5944	3.08239	.48139

Independent Samples Test

		Levene's Test for Equality of Variances		t-test for Equality of Means						
		F	Sig.	t	df	Sig. (2-tailed)	Mean Difference	Std. Error Difference	95% Confidence Interval of the Difference	
									Lower	Upper
MTR	Equal variances assumed	16.373	.000	-1.634	74	.106	-1.71439	1.04911	-3.80480	.37602
	Equal variances not assumed			-1.562	49.727	.125	-1.71439	1.09758	-3.91925	.49047



SCOLEX

		Frequency	Percent	Valid Percent	Cumulative Percent
Valid	PRESENT	33	43.4	94.3	94.3
	ABSENT	2	2.6	5.7	100.0
	Total	35	46.1	100.0	
Missing	System	41	53.9		
Total		76	100.0		

Demonstration of scolex within a cyst in CT/MRI is considered the absolute criteria for the diagnosis of Neurocysticercosis as per the Revised diagnostic criteria of NCC. ps3d / 3d CISS sequence was used and images obtained demonstrate scolex in a better way. In two patients, scolex was not seen. In both patients, scolex was demonstrated in previous imaging studies done 1-2 months

before. Both were on Anti parasite treatment. Scolex was demonstrated in 94.3% of patients with Neurocysticercosis.

Discussion

The study population included patients from 6yrs to 72yrs. Majority of the patients were less than 40yrs of age.

41 tuberculoma in 21 patients were analyzed. 8 patients had multiple tuberculoma. 4 patients had miliary pulmonary tuberculosis. One patient had caries spine. Rest of the patients had positive chest x-ray for pulmonary tuberculosis. 13 patients had solitary lesions in brain and had typical features of tuberculoma in conventional MRI. Follow up after 2 months showed clinical improvement and reduction in the size of the lesion or the surrounding vasogenic edema.

MTR was calculated from the rim of the lesion. Mean MTR was 16.6 ± 3.7 .

In the study of Rakesh Gupta et al (8), it is stated there was no significant difference between the MT ratios in the core and the rim of Tuberculous lesions.

Tuberculoma were better seen in precontrast MT SE images compared to T1WI and T2WI. Visibility of the lesion on MT-SE images depends on the difference in contrast between brain parenchyma and the lesion due to differential transfer of magnetization. T2 hypointense Tuberculomas are prominent on precontrast MT-SE images. Detection of conventional SE-invisible tuberculomas on MT-SE images is the result of the lower transfer of magnetization in granulomas as compared with surrounding brain parenchyma.

Detectability of more lesions on precontrast MT-SE images that do not enhance after contrast injection suggests a lack of breach of the bloodbrain barrier in some of the lesions. Disruption of the blood-brain barrier depends on the activity of the lesion and inactive lesions may not enhance after contrast administration (8).

Precontrast MT-SE images help in judging the enhancement of the lesion on post contrast MT-SE images by comparison between the increase in signal intensity of lesion in pre and post contrast images. Post contrast MT-SE images alone may give a false impression of contrast enhancement of all the MT hyper intense lesions, even when there is no breach in the blood-brain barrier (8).

One patient had associated lacunar infarct in basal ganglia. Two study patients also had basal meningitis. In precontrast MTSE images, periparenchymal hyper intensity along the surface of brain stem was visible. On contrast, there was enhancement of the basal meninges and cisternal tuberculoma. (Fig). In tuberculous meningitis, tuberculomas along with the exudates are found in the meninges, which are composed of cellular infiltrate, degenerated and partly caseated fibrin, tubercles, and, rarely, bacilli (8). These were probably responsible for the differential MT ratio between brain parenchyma and inflamed meninges, and hence its visibility on precontrast MT-SE images. The MT ratio of inflamed

meninges with exudates in tuberculosis meningitis is significantly lower than other causes of Meningitis. (8)

Using MT Ratio of 16.6 ± 3.7 (12.9 – 20.3), the sensitivity for detecting tuberculoma was 78%, specificity was 73% and positive predictive value was 78%.

35 Neurocysticercus lesions were analyzed in 22 patients. The size of the lesion ranged from 8mm to 15.5mm. Intra ventricular cysts were larger in size.

Demonstration of scolex within a cyst in CT/MRI is considered the absolute criteria for the diagnosis of Neurocysticercosis as per the Revised diagnostic criteria of NCC. ps3d / 3d ciss sequence was used and images obtained demonstrate scolex in a better way. In two patients, scolex was not seen. In both patients, scolex was demonstrated in previous imaging studies done 1-2 months before. Both were on Anti parasite treatment. Cyst wall and scolex of intraventricular cysts were better seen with ps3d / 3d ciss sequence The increased sensitivity of the 3D-CISS sequence is a consequence of its higher resolution and may also be related to accentuation of the T2 value between the cystic fluid and surrounding CSF.

Degenerating NCC cysts show hypo intense center with hyper intense rim in MT images. There were 21 cystic lesions (representing vesicular stage of NC) which showed MTR of 10.9 ± 2.8 (9.6 – 12.18). There were 3 granuloma which were hypointense on T2WI which showed MTR which was significantly higher

(23.725 ± 3). 14 lesions with imaging features suggestive of degenerative cysts showed MTR of 20.8 ± 3.5 ($18.7 - 22.9$).

According to the study of Rakesh Gupta et al, the tuberculous lesions with a hypointense core on T2-weighted images had MT ratios of 23.8 ± 1.76 in the rim and 24.2 ± 3.1 in the core. In this study, the mean MTR was 16.6 ± 3.7 for Tuberculoma.

There are several key parameters in the off-resonance saturation transfer technique that can alter the quantitative and qualitative MTR. The principle determinants being the base sequence used, characteristics of the saturating pulse (pulse type, power, duration, time between pulses, duty cycle i.e. number of pulses per TR, bandwidth, its effective flip angle), offset frequency of the saturating pulse, and field strength. All of these characteristics alter the degree of saturation and Magnetization transfer ratio obtained and must be known before quantitative comparisons can be made between clinical studies. (28). So, machine parameters could be the reason for the variability of MTR measured in both studies.

The number of patients enrolled in this study was less than the previous study conducted. This could account for the wide confidence interval noticed in this study.

Limitations

1. Total lesions analysed include 41 tuberculoma and 35 Neurocysticercus. A total of 107 tuberculomas in seven patients were analyzed in the study by Rakesh Gupta et al (8). The no of patients enrolled in this study was less than the previous study conducted. This could account for the wide confidence interval noticed in this study.
2. Magnetization transfer ratio obtained for white and grey matter as well as tuberculoma and NCC were less than the previous studies. This is probably due to technical and machine parameters. Hence MTR has to be standardized for each machine and MTR between two different studies cannot be compared.
3. Histopathological results are available for only one lesion.

Magnetization transfer ratio can be used to differentiate tuberculoma and T2 hypointense neurocysticercosis. Demonstration of scolex using ps3d or 3d CISS sequence can be used to diagnose innocuous cystic lesion and T2 hyperintense NCC.

Conclusion:

1. MT ratio can be used to differentiate T2 hypointense NCC and Tuberculoma.

MT Ratio of Tuberculoma is 16.6 ± 3.1

MT Ratio of T2 hypointense NCC is 23.725

2. Demonstration of scolex in NCC (an absolute criteria for diagnosis of NCC) can be done by using ps3d / CISS sequence especially useful in intraventricular Neurocysticercosis.
3. T2 invisible Tuberculomas are better visualized in MT images. Hence disease load can be better assessed using MT images.
4. Presence of associated meningeal disease can be demonstrated using precontrast MT SE Images in Tuberculoma.

Bibliography

1. Ravindra Kumar Garg et al, Single Enhancing Computerized Tomography-Detected Lesion in Immunocompetent Patient, Journal of Neurosurgery June 2002 Volume 12, Number 6.
2. AP Jain, Rajnish Joshi, Tejal Lathia, Single Small Enhancing Computed Tomography Lesion: A Review, JIACM 2005; 6(2): 114-21.
3. Rajshekhar V, Haran RP, Prakash GS, et al, Differentiating solitary small cysticercus granulomas and tuberculomas in patients with epilepsy. Clinical and computerized tomographic criteria, J Neurosurg 78:402-407, 1993.
4. Chopra JS, Sawhney IMS, Suresh N, et al: Vanishing CT lesions in epilepsy. J Neurol Sci 107:40-49, 1992
5. Garg RK, Nag D: Single enhancing CT lesions in Indian patients with seizures: clinical and radiological evaluation and follow-up. J Trop Pediatr 44:204-210, 1998
6. Garg RK, Singh MK, Misra S: Single-enhancing CT lesions in Indian patients with seizures: a review. Epilepsy Res 38: 91-104, 2000
7. Rajshekhar V: Rate of spontaneous resolution of a solitary cysticercus granuloma in patients with seizures. Neurology 57: 2315-2317, 2001.

8. Rakesh K. Gupta, Manoj K. Kathuria, and Sunil Pradhan, Magnetization Transfer MR Imaging in CNS Tuberculosis; *AJNR Am J Neuroradiol* 20:867–875, May 1999.
9. J.M.K Murthya, Ravi Yangalab, Acute symptomatic seizures — incidence and etiological spectrum: a hospital-based study from South India, Volume 8, Issue 3, Pages 162-165 (May 1999).
10. Chandy MJ, Rajshekhar V, Prakash S, et al: Cysticercosis causing single, small CT lesions in Indian patients with seizures. *Lancet* 1:390–391, 1989
11. Anne G. Osborn, *Diagnostic Neuroradiology* .
12. Anne G. Osborn, *Diagnostic imaging brain*, first edition.
13. Rakesh K. Gupta, N. Husain, M.K. Kathuria, S. Datta, R.K.S. Rathore, M. Husain, Magnetization Transfer MR Imaging Correlation with Histopathology in Intracranial Tuberculomas; *Clinical Radiology*, Volume 56, and Issue 8, Pages 656-663.
14. J. M. K. Murthy, Ravi Yangala , Mantha Srinivas, *Epilepsia The Syndromic Classification of the International League Against Epilepsy: A Hospital-Based Study from South India*; Volume 39 Issue 1, Pages 48 – 54.
15. Mutasem Abuhamed, Xiao Bo and Cai Yan, Central Nervous System Tuberculomas: A Review Article *American Journal of Infectious Diseases* 4 (2): 168-173, 2008.

16. Robert I. Grossman, MD, John M. Gomori, MD, Karen N. Ramer, BA, Frank J. Lexa, MD, Mitchell D. Schnall, MD, PhD, Magnetization Transfer: Theory and Clinical Applications in Neuroradiology; *RadioGraphics* 1994; 14:279-290
17. Pulsed Magnetization Transfer Imaging : Evaluation Of Technique Simon J Graham, PhD, R Mark Henkeiman, PhD; *Radiology* 1999; 202 903 – 910
18. Jinkins JR, Gupta R, Chang KH, Carbajal JR. MR imaging of central nervous system tuberculosis. *Radiol Clin North Am* 1995;33:771–786
19. Poptani H, Gupta RK, Roy R, Pandey R, Jain VK, Chhabra DK. Characterization of intracranial mass lesions with in vivo proton MR spectroscopy. *AJNR Am J Neuroradiol* 1995;16:1593– 1603
20. Mehta RC, Bruce Pike G, Enzmann DR. Magnetization transfer MR of the normal adult brain. *AJNR Am J Neuroradiol* 1995; 16:2085–2091
21. Edelman RR, Ahn SS, Chien D, et al. Improved time-of-flight MR angiography of the brain with magnetization transfer contrast. *Radiology* 1992;184:395–399
22. Wolff S, Balaban R. Magnetization transfer contrast (MTC) in magnetic resonance imaging. *Magn Reson Med* 1989;10:135–144
23. Balaban RS, Ceckler TL. Magnetization transfer contrast in magnetic resonance imaging. *Magn Reson Q* 1992;8:116–137
24. Yeung HN AA. Magnetization transfer contrast with periodic pulsed saturation; *Radiology* 1992;183:209–2147.

25. Muller RN, Marsh MJ, Bemardo MI, Lauterbur PC. True 3-D imaging of limbs by NMR zeugmatography with off-resonance irradiation. *Eur J Radiol* 1983; 3:286-290.
26. Wolff SD, Balaban RS. Magnetization transfer contrast (MTC) and tissue water proton relaxation in vivo. *Magn Reson Med* 1989; 10:135-144.
27. Wolff SD, Eng J, Balaban RS. Magnetization transfer contrast: method for improving contrast in gradient-recalled-echo images. *Radiology* 1991;179:133-137.
28. R Gupta, 2002, Magnetization transfer MR imaging in central nervous system infections, *Indian Journal of Radiology and Imaging* Volume : 12, Issue : 1, Page : 51-58
29. Agarwal A, Raghav S, Husain M, Kumar R, Gupta RK. Epilepsy with focal cerebral calcification: Role of magnetization transfer MR imaging. *Neurol India* 2004;52:197-9.
30. Central Nervous System Tumor, Infection, and Infarction: Detection with Gadolinium-enhanced Magnetization Transfer MR Imaging' *Radiology* 1995; 195:41-46.
31. Gupta RK, Roy R, Poptani H, et al. Finger printing of *Mycobacterium tuberculosis* in intracranial tuberculomas using in vivo, ex vivo and in vitro proton MR spectroscopy. *Magn Reson Med* 1996;36:829-833.

32. Woff SD, Balaban RS. Magnetization transfer contrast (MTC) and tissue water proton relaxation in vivo. *Magn Reson Med* 1989;10:135–144.
33. Rakesh K Guptaa, Mazhar Husainb, Devendra K Vatsalb, Rajesh Kumara, Sanjeev Chawlaa, Nuzhat Husain, Comparative evaluation of magnetization transfer MR imaging and in-vivo proton MR spectroscopy in brain tuberculomas; *Magnetic resonance imaging*, volume 20, Issue 5, Pages 375-381 (June 2002).
34. Kathuria MK, Gupta RK, Roy R, Gaur V, Husain N, Pradhan S. Measurement of magnetization transfer in different stages of neurocysticercosis; *J Magn Reson Imaging* 1998;8:473–479.
35. R.Gupta, Comparative evaluation of magnetization transfer MR imaging and in-vivo proton MR spectroscopy in brain tuberculomas, *Magnetic Resonance Imaging*, Volume 20, Issue 5, Pages 375-381.
36. Praphan Yodnopaklow and Arunee Mahuntussanapong Single small enhancing CT lesion in Thai patients with acute symptomatic seizures: a clinico-radiological study, *Tropical Medicine and International Health* volume 5 no 4 pp 250–255 april 2000
37. Grainger & Allison's *Diagnostic Radiology*, fifth edition.
38. P Kamra, Md, R Azad, Md, K N Prasad, Md, S Jha, Md, S Pradhan, Md And R K Gupta, Infectious meningitis: prospective evaluation with magnetization transfer MRI; *The British Journal Of Radiology*, 77 (2004), 387–394.

39. Wasay M, Kheleani BA, Moolani MK, Zaheer J, Pui M, Hasan S, et al. Brain CT and MRI findings in 100 consecutive patients with intracranial tuberculoma. *J Neuroimaging* 2003;13:240-7.
40. M. K. Vasudev, P. N. Jayakumar, S. G. Srikanth, K. Nagarajan and A. Mohanty Quantitative Magnetic Resonance Techniques in the Evaluation of Intracranial Tuberculomas: *Acta radiologica* 2007, Vol. 48, No. 2, Pages 200-206
41. Rakesh K. Gupta, Davender K. Vatsal, Nuzat Husain, Sanjeev Chawla, Kashi N. Prasad, Raja Roy, Rajesh Kumar, Deepak Jha and Mazhar Husain, Differentiation of Tuberculous from Pyogenic Brain Abscesses with In Vivo Proton MR Spectroscopy and Magnetization Transfer MR Imaging; *American Journal of Neuroradiology* 22:1503-1509 (9 2001).
42. Intracranial tuberculomas: MRI signal intensity correlation with histopathology and localised proton spectroscopy. Gupta RK, Pandey R, Khan EM, Mittal P, Gujral RB, Chhabra DK. *Magn Reson Imaging*. 1993;11(3):443-9.
43. Comparative evaluation of magnetization transfer contrast and fluid attenuated inversion recovery sequences in brain tuberculoma. Saxena S, Prakash M, Kumar S, Gupta RK. *Clin Radiol*. 2005 Jul;60(7):787-93.
44. Tae Kyoung Kim, Kee Hyun Chang, Chong Jai Kim, Jin Mo Goo, Myeong Cherl Kook, and Moon Hee Han; Intracranial Tuberculoma: Comparison of MR

with Pathologic Findings; AJNR 16:1903–1908, Oct 1995 0195-6108/95/1609–1903.

45 Khanna PC, Godinho S, Patkar DP, Pungavkar SA, Lawande MA. MR spectroscopy-aided differentiation:"Giant" extra-axial tuberculoma masquerading as meningioma; AJNR Am J Neuroradiol 2006;27:1438-40.

46. Shindo A, Honda C, Baba Y. A case of an intracranial tuberculoma, mimicking meningioma that developed during treatment with anti-tuberculous agents. No Shinkei Geka 1999;27:837-41

47. Bauer J, Johnson RF, Levy JM, Pojman DV, Ruge JR. Tuberculoma presenting as an en plaque meningioma. Case report. J Neurosurg 1996;85:685-8.

48. Cysticercosis and Epilepsy: A Critical Review, Arturo Carpio et al

49. Neurocysticercosis: Updates on Epidemiology, Pathogenesis, Diagnosis, and Management. Annual Review of Medicine Vol. 51: 187-206 (Volume publication date February 2000)

50 Professor Arturo Carpio a et al., The Lancet Infectious Diseases, Volume 2, Issue 12, Pages 751 - 762, December 2002 Neurocysticercosis: an update.

51. V. Rajshekhar, MCh et al, Active epilepsy as an index of burden of neurocysticercosis in Vellore district, India.

52. A Kuruvilla, J D Pandian, M Nair, V V Radhakrishnan, S Joseph, Neurocysticercosis: A Clinical and Radiological Appraisal from Kerala State, South India; Singapore Med J 2001 Vol 42(7) : 297-303.
54. Del Brutto OH, Rajshekhar V, White AC Jr, et al. Proposed diagnostic criteria for neurocysticercosis. Neurology 2001;57:177-83.
55. Garg RK. Diagnostic criteria for neurocysticercosis: some modifications are needed for Indian patients. Neurol India 2004;52(2):171-7.
56. Edneia c. bueno, Application of synthetic 8-kd and recombinant gp50 antigens in the diagnosis of neurocysticercosis by enzyme-linked immunosorbent assay.
57. Professor Arturo Carpio a et al, The Lancet Infectious Diseases, Neurocysticercosis: an update; Volume 2, Issue 12, Pages 751 - 762, December 2002.
58. HR Martinez et al., MR imaging in neurocysticercosis: a study of 56 cases ; American Journal of Neuroradiology, Vol 10, Issue 5 1011-1019.
59. Rajshekhar V, Chandy MJ. Validation of diagnostic criteria for solitary cysticercus granuloma in patients presenting with seizures. Acta Neurol Scand 1997;96:76-81.
60. Srikanth Subbamma Govindappa et al, Improved Detection of Intraventricular Cysticercal Cysts with the Use of Three-dimensional Constructive Interference in Steady State MR Sequences; AJNR Am J Neuroradiol 21:679–684, April 2000.

61. Serpa, Jose A; Yancey, Linda S; White Jr, A Clinton, Expert Review of Anti-Infective Therapy, Volume 4, Number 6, December 2006 , pp. 1051-1061.
62. Vedantam Rajshekhar, MCh and Lakshmanan Jeyaseelan, PhD, Seizure outcome in patients with a solitary cerebral cysticercus granuloma.
63. R.Gupta, M.Prakash, A.Mishra, M.Husain, K.Prasad, N.Husain, Role of diffusion weighted imaging in differentiation of intracranial tuberculoma and tuberculous abscess from cysticercus granulomas-a report of more than 100 lesions European Journal of Radiology, Volume 55, Issue 3, Pages 384-392.
64. Vedantam Rajshekhar, M.Ch., R. P. Haran, M.Ch., G. Shankar Prakash, M.Ch., and Mathew J. Chandy, M.S.(Gen), M.Ch, Differentiating solitary small cysticercus granulomas and tuberculomas in patients with epilepsy Clinical and computerized tomographic criteria; March 1993 Volume 78, Number 3
65. L.T. Lucato M.S. Guedes J.R. Sato L.A. Bacheschi L.R. Machado C.C. Leite, The Role of Conventional MR Imaging Sequences in the Evaluation of Neurocysticercosis: Impact on Characterization of the Scolex and Lesion Burden; AJNR Am J Neuroradiol 28:1501– 04 _ Sep 2007.
66. O. H. Del Brutto, MD;, V. Rajshekhar, MCh;, A. C. White Jr., MD;, V. C. W. Tsang, PhD;, T. E. Nash, MD;, O. M. Takayanagui, MD;, P. M. Schantz, DVM, PhD;, C. A. W. Evans, MD;, A. Flisser, DSc;, D. Correa, DSc;, D. Botero, MD;, J. C. Allan, PhD;, E. Sarti, MD, DSc;, A. E. Gonzalez, DVM, PhD;, R. H. Gilman,

MD; and H.H. García, MD; Proposed diagnostic criteria for neurocysticercosis, *Neurology* 2001;57:177-183.

67. Hector H. García, Carlton A. W. Evans,^{3,4} Theodore E. Nash,⁵ Osvaldo M. Takayanagui,⁶ A. Clinton White, Jr.,⁷ David Botero,⁸ Vedantam Rajshekhar,⁹ Victor C. W. Tsang,¹⁰ Peter M. Schantz,¹⁰ James C. Allan,¹¹ Ana Flisser,¹² Dolores Correa,¹³ Elsa Sarti,¹⁴ Jon S. Friedland,⁴ S. Manuel Martinez,¹ Armando E. Gonzalez,¹⁵ Robert H. Gilman,^{1,2,16} and Oscar H. Del Brutto¹⁷; Current Consensus Guidelines for Treatment of Neurocysticercosis ; *Clinical Microbiology Reviews*, Oct. 2002, p. 747–756 Vol. 15, No. 4 .

68. Rajshekhar V, Chandy MJ. Validation of diagnostic criteria for solitary cysticercus granuloma in patients presenting with seizures. *Acta Neurol Scand* 1997;96:76-81.

Proforma

1. NAME

2. AGE

3. SEX

4. CLINICAL PROFILE

5. MRI BRAIN

NO OF LESIONS,

SIZE	LOCATION	T1	T2	T1	MT	MTR	CISS
------	----------	----	----	----	----	-----	------

6. OTHER INVESTIGATION

7. Follow up

